Crawford et al. Supplemental Figure 1

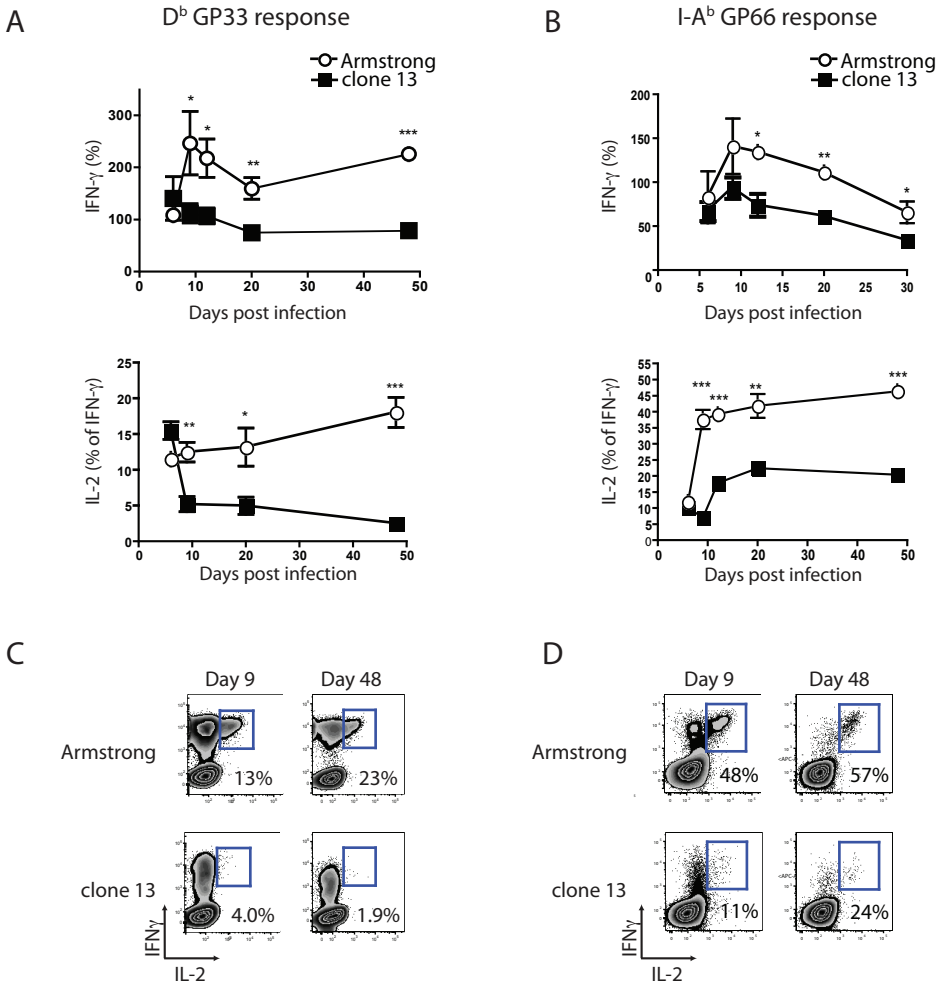

Supplemental Figure 1. Exhausted CD4⁺ and CD8⁺ T cells produce less IFN-γ and IL-2 throughout the response to clone 13 compared to Armstrong infection. (A) Graphs show the percent of D^bGP33-specific CD8⁺ T cells making IFN-γ after Arm (open circles) versus clone 13 infection (close squares) (top) following peptide stimulation in vitro and the percentage of IFN-γ producing cells also co-producing IL-2 (bottom). (B) Graphs show percentage of I-A^bGP66-specific CD4⁺ T cells making IFN-γ after Arm (open circles) versus clone 13 infection (close squares) (top) following peptide stimulation in vitro and the percentage of IFN-γ producing cells also co-producing IL-2 (bottom). (C and D) Representative flow cytometry plots are shown for IFN-γ and IL-2 co-production in response to GP33-41 (C) or GP66-77 peptide stimulation (D). **Figure S1** related to **Figure 1.**

Crawford et al. Supplemental Figure 2

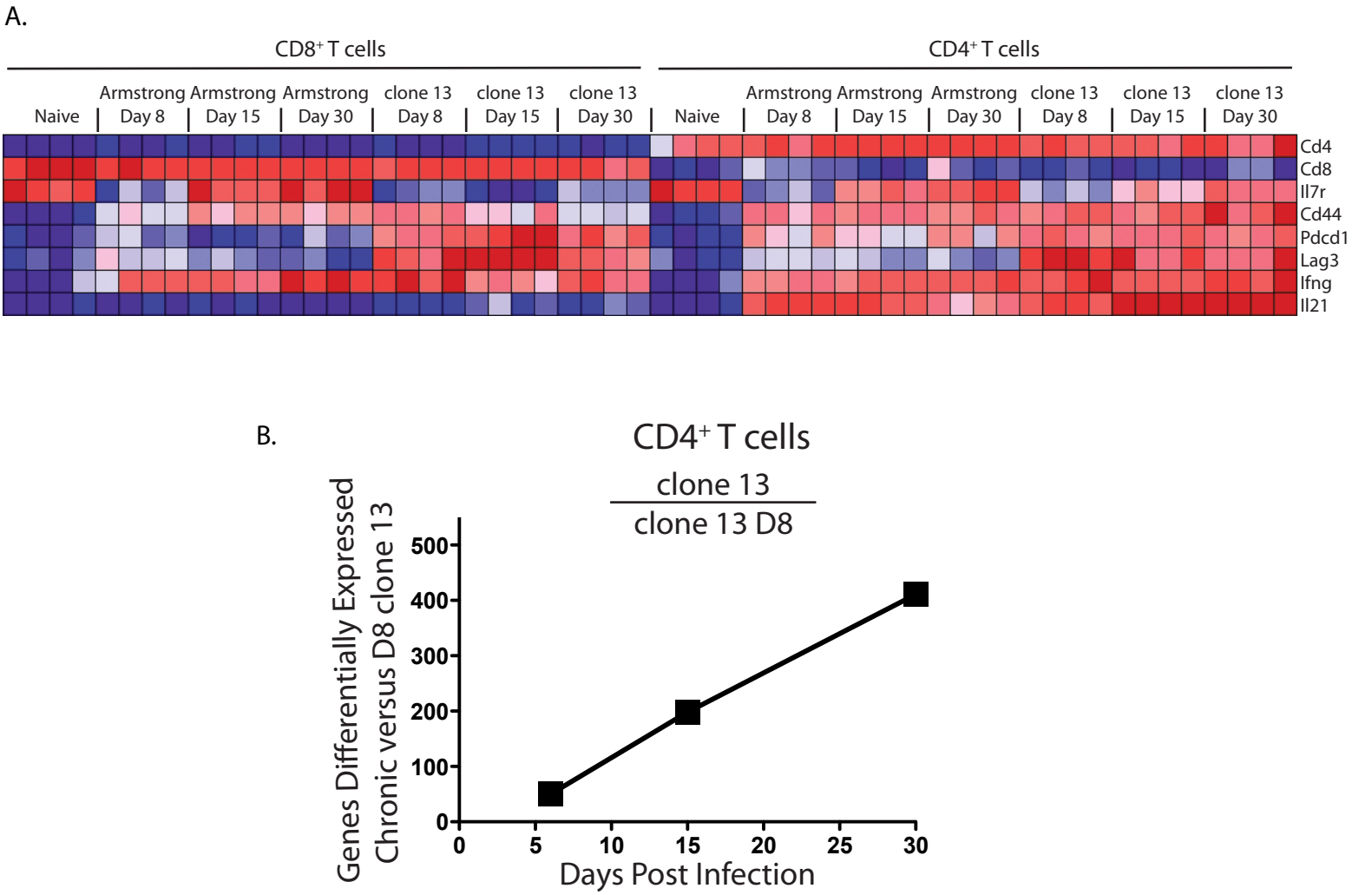

Supplemental Figure 2. Examination of selected gene expression for microarray validation.
(A) A heat map is shown of the expression of selected genes from the microarray. These genes are known to change in effector, memory or exhausted T cells. (B) Graph shows the total number of differentially expressed genes in CD4 T cells from clone 13-infected mice at day 6, 15 and 30 p.i. compared to cells isolated at d8 p.i. with clone 13.
Figure S2 related to **Figure 2**.

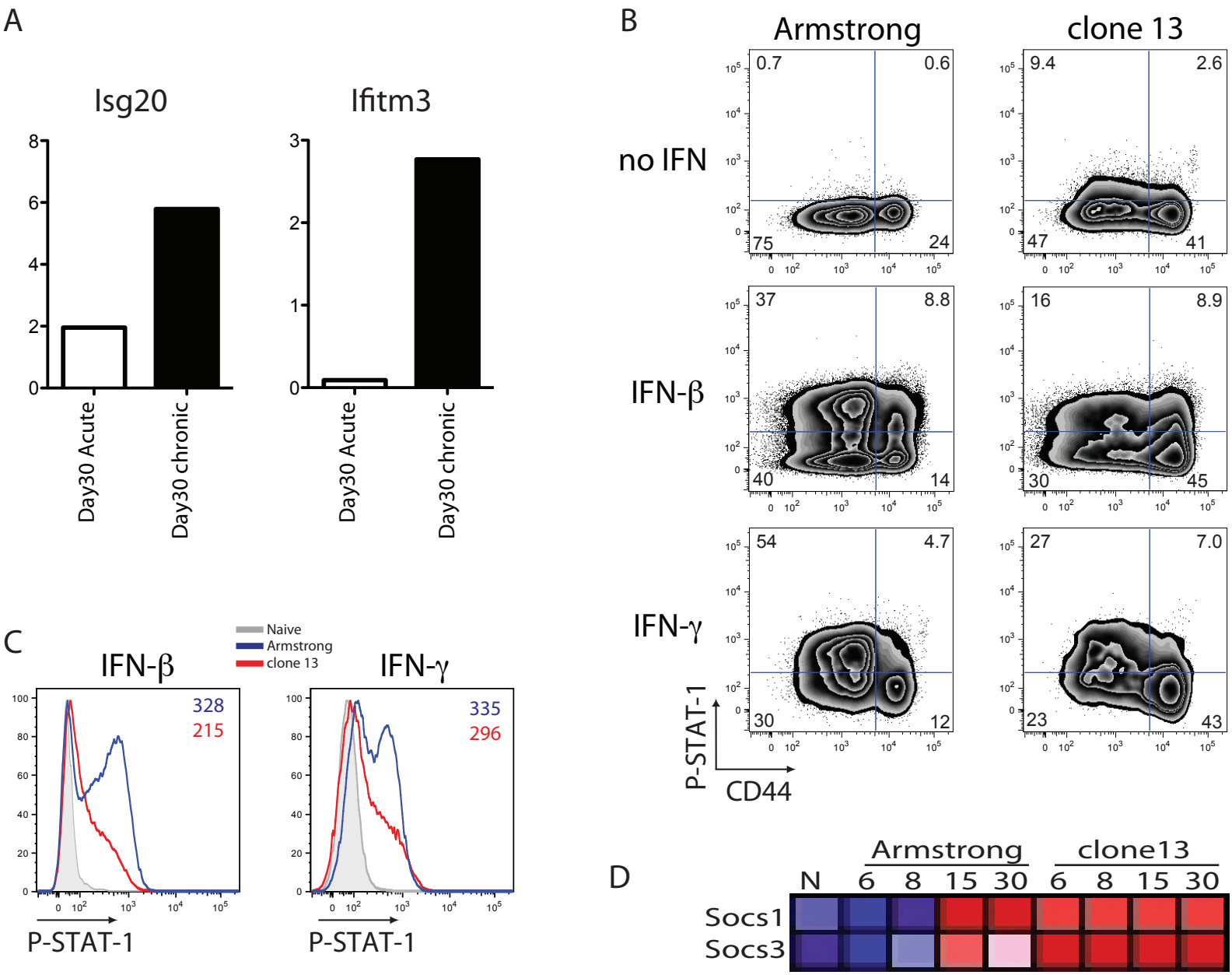

Supplemental Figure 3. IFN-responsive genes are upregulated in exhausted CD4⁺ T cells but exhausted CD4⁺ T cells are less responsive to IFNs

C57Bl/6 mice were infected with Arm or clone 13 and sacrificed on d30 p.i. (A) I-A^b GP66-specific CD4⁺ T cells were sorted directly into trizol to examine mRNA expression. Graphs show the fold change in mRNA expression of Isg20 and Ifitm3 in memory or exhausted CD4⁺ T cells. (B) Spleens from mice on d30 p.i. with Arm or clone 13 were cultured in the presence or absence of IFN-β1 or IFN-γ for 15 minutes and phosphorylated STAT-1 examined by flow cytometry. Representative flow cytometry plots of CD44 versus pSTAT-1 staining in memory and exhausted after 15 minutes of incubation with IFN. Gated on total CD4⁺ T cells. (C) Representative histograms are shown for pSTAT-1 staining following stimulation with IFN-β or IFN-γ as above. Gated on total CD4⁺ T cells. Grey histograms are unstimulated cells from Arm infection, Blue histograms are cells from Arm infection and Red histograms are cells from clone 13 infection. Numbers indicate MFI of pSTAT-1. (D) Relative mRNA expression of Socs1 and Socs3 in CD4 T cells are shown as a heatmap.
Figure S3 related to **Figure 3**.

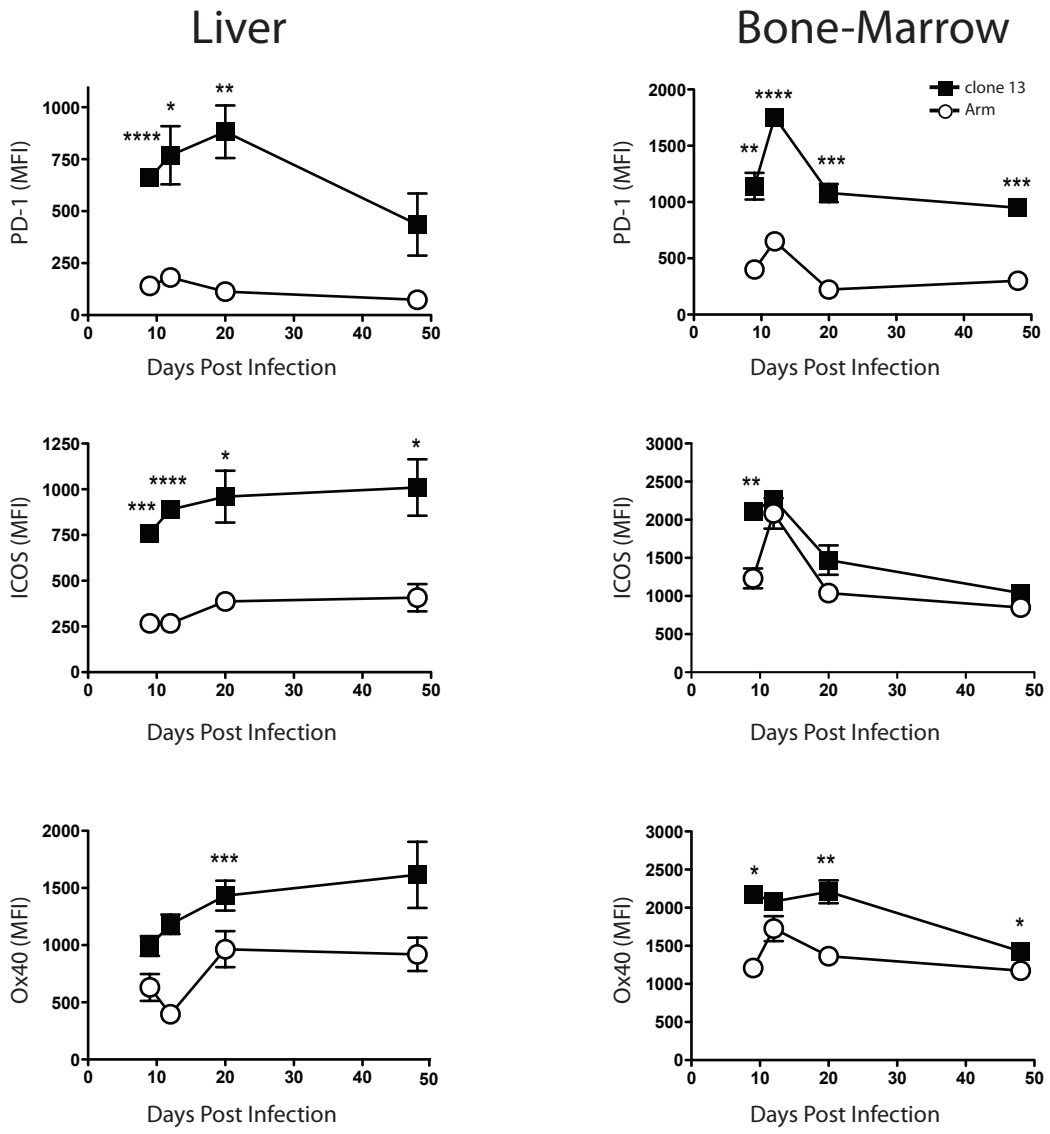

Supplemental Figure 4. Similar expression of inhibitory and costimulatory molecules can be seen in multiple tissues during chronic LCMV infection.
I-A^{b}GP66-specific CD4^{+} T cells were examined for expression of PD-1, ICOS and OX40 on various days p.i. with LCMV Arm of clone 13. **Figure S4** related to **Figures 4** and **5**.

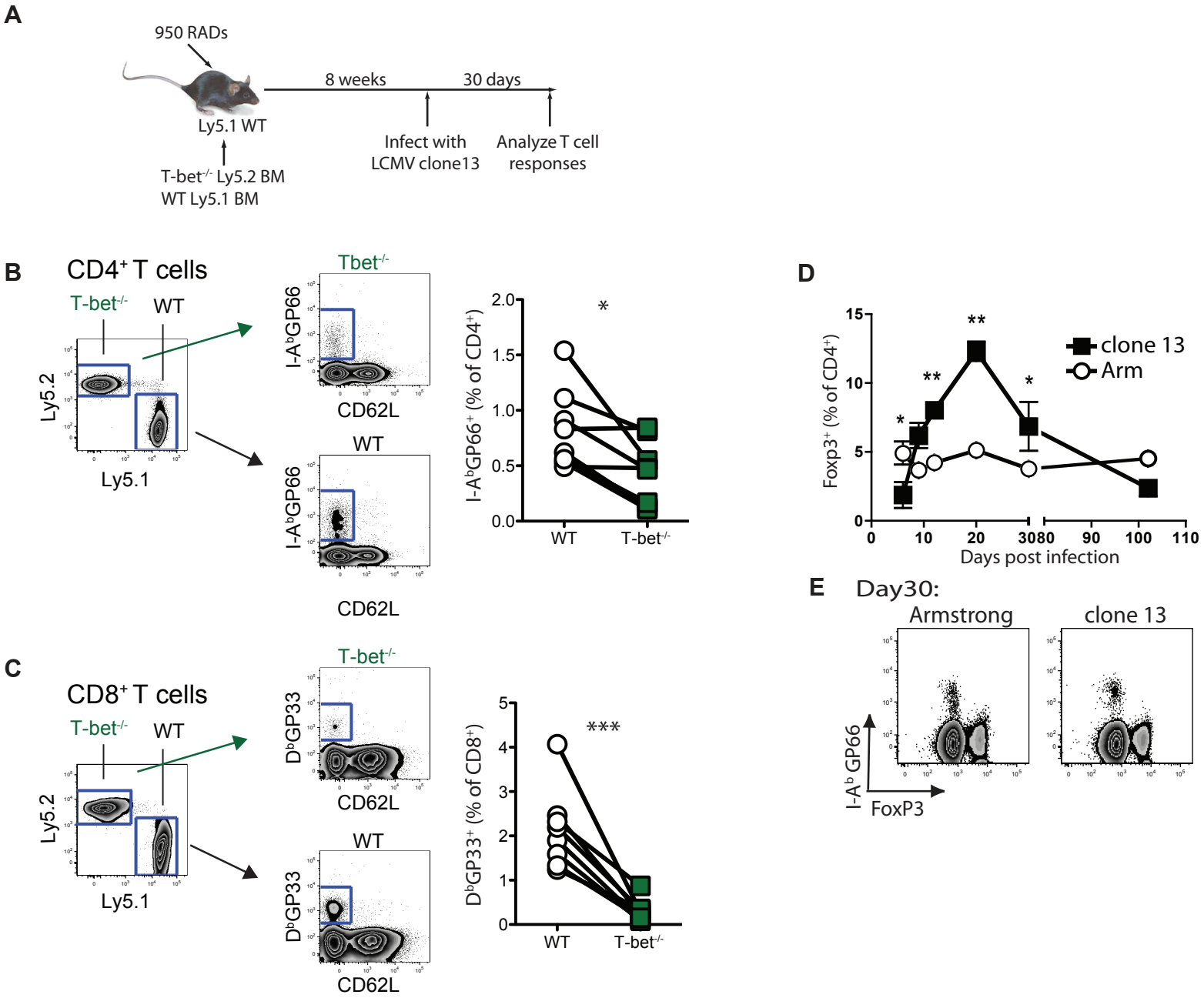

Supplemental Figure 5. T-bet and Foxp3 in CD4+ T cells responding to clone 13 infection.
(A) Bone-marrow chimeras were made where 50% of the cells were WT (Ly5.1+) and 50% were T-bet$^{-/-}$. After 8 weeks of reconstitution, mice were infected with LCMV clone 13 and the T cell responses examined. (B) Representative flow cytometry plots are shown. Graph shows the percentage of CD4^{+} T cells that are I-A^{b} GP66-specific of WT (open circles) or T-bet$^{-/-}$ (green squares) CD4^{+} T cells. (C) Representative plots showing percentage of CD8+ T cells that are D^{b}GP33-specific in the same mixed chimeras. (D) Mice were infected with Arm or clone 13 and sacrificed on the indicated days to determine the proportion of Treg cells based on FoxP3 staining. Graphs shows the percentage of CD4^{+} T cells that are FoxP3^{+} on indicated days. (E) Representative flow cytometry plots of I-A^{b}GP66-77 versus Foxp3 staining on day 30 p.i. with Arm or clone 13. **Figure S5** related to **Figure 6**.

Crawford et al Supplemental Figure 6

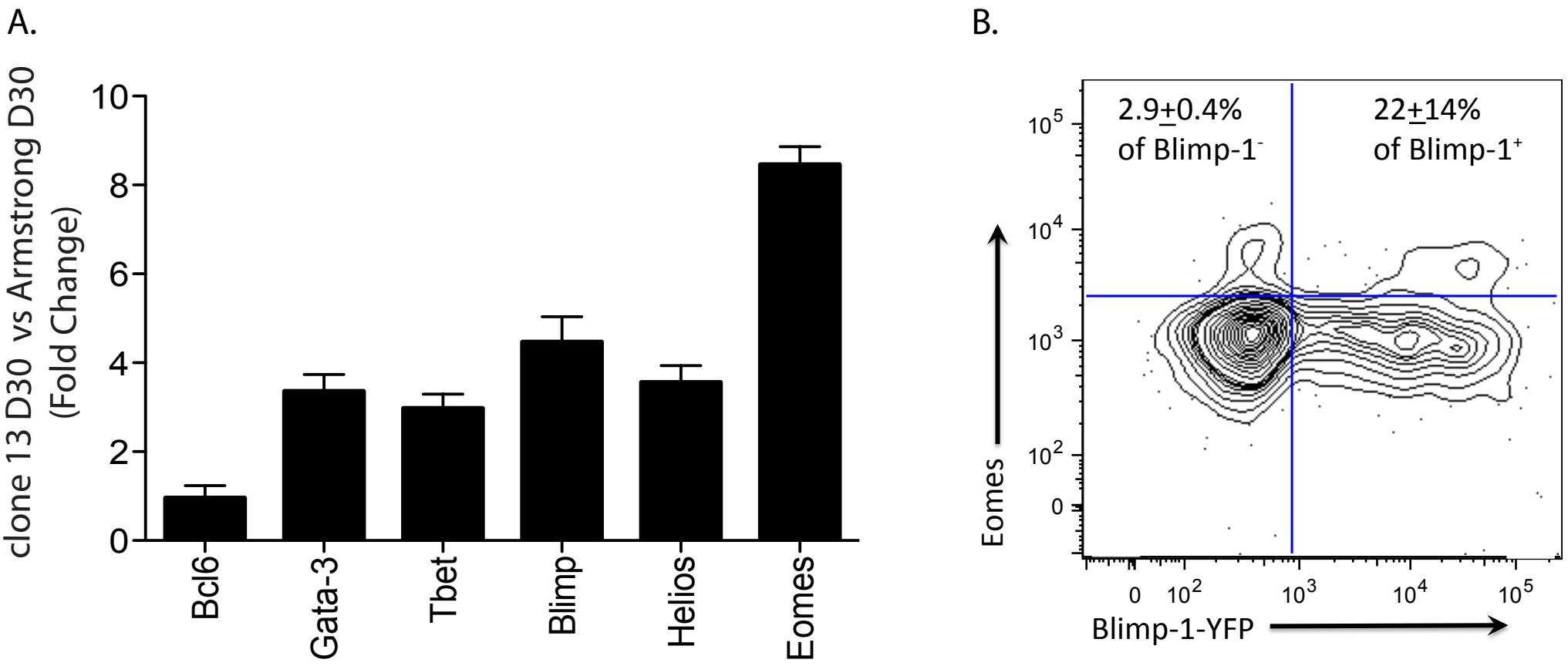

Supplemental Figure 6. Multiple lineage-specific transcription factors are upregulated in CD4⁺ T cells responding to clone 13 infection and co-expression of transcription factors defines subsets of LCMV-specific CD4⁺ T cells during chronic infection.
(A) C57Bl/6 mice were infected with Arm or clone 13. Thirty days later, I-A^{b}GP66-specific CD4⁺ T cells were sorted from splenocytes and mRNA expression was analyzed by RT-PCR for the genes Bcl6, Gata3, Tbx21 (T-bet), Prdm1 (Blimp-1), Ikzf2 Helios and Eomes. Graphs show the mean fold change (±SD) in exhausted versus memory CD4⁺ T cells. **(B)** Blimp-1-YFP mice were infected with clone 13. Thirty days later, I-A^{b}GP66-tetramer⁺ CD4⁺ T cells were examined by flow cytometry for co-expression of Blimp-1-YFP and Eomes. Plot is gated on live, B220⁻ NK1.1⁻ CD8⁻ CD4⁺ tetramer⁺ cells. Numbers represent summary data from 4 mice. Representative of at least 2 independent experiments. **Figure S6** related to **Figure 7.**

Supplemental Experimental Procedures

Antibodies for surface and intracellular staining

For *ex vivo* surface and intracellular staining, the following antibodies were used: CD44 Alexa Fluor 700, Helios FITC, PD-1 PE-Cy7, BTLA PE, ICOS PerCP-Cy5.5, CD28 Pe-Cy7, CD27 PerCP-Cy5.5 (all Biolegend), Eomes PE, FoxP3 Pe-Cy7, LAG-3 PE, CD160 PE, GL7 Alexa Fluor 488, Bcl6 PE (Ebioscience), CTLA-4 PE, 2B4 FITC and CXCR5-biotin (BD Biosciences), Tbet FITC (Santa cruz) and OX40 FITC (Abcam). For ICS, the following antibodies were used: IFNγ APC, IL-2 PE, MIP-1α PE, IL-10 APC, IL-4 PE or IL-17 PE (BDbiosciences) and TNFα Pacific Blue (Biolegend).